IOP Publishing Semiconductor Science and Technology
Semicond. Sci. Technol. **29** (2014) 015006 (10pp) doi:10.1088/0268-1242/29/1/015006

# Graphite/CdMnTe Schottky diodes and their electrical characteristics

**L A Kosyachenko[1], R Yatskiv[2], N S Yurtsenyuk[1], O L Maslyanchuk[1] and J Grym[2]**

[1] Chernivtsi National University, 58012 Chernivtsi, Ukraine
[2] Institute of Photonics and Electronics, Academy of Sciences CR, v.v.i., Chaberska 57, CZ-18251 Prague 8, Czech Republic

E-mail: lakos@chv.ukrpack.net

Received 2 September 2013, revised 14 October 2013
Accepted for publication 29 October 2013
Published 4 December 2013

**Abstract**

The first Schottky diodes based on n-CdMnTe crystals with pronounced rectifying properties are investigated. It is shown that the *I–V* characteristics of the diodes fabricated by printing colloidal graphite can be described by the Sah–Noyce–Shockley theory of generation–recombination in the space charge region. Exponential increase of forward current with voltage is limited by a relatively low barrier height at the graphite/CdMnTe contact ($\sim 0.4$ eV) and a significant series resistance of the crystal bulk ($\sim 10^6$ Ω at room temperature). Tunneling due to high concentration of uncompensated impurities in investigated $Cd_{0.9}Mn_{0.1}Te$ crystals ($7 \times 10^{17}$ cm$^{-3}$) does not allow increasing the reverse bias voltage to the values needed for the operation of *x*- and $\gamma$-ray detectors. High concentration of uncompensated donors is interpreted by the fact that a certain part of the Mn atoms does not substitute for Cd but plays a role of over-stoichiometric impurities. In the case of the presence of a thin intermediate insulator layer in the graphite/CdMnTe contact, a rapid increase in the current for both polarities of high voltage due to the Frenkel–Poole emission is observed. The obtained results shed light on the problems of technology of growing and post-processing CdMnTe crystals regarded as a prospective material for *x*- and $\gamma$-ray detectors.

(Some figures may appear in colour only in the online journal)

## 1. Introduction

CdTe is the basic material for efficient *x*- and $\gamma$-ray detectors operating without cryogenic cooling and is widely used in science, industry and other application areas. To date, the technology of growing the CdTe crystals with high resistivity $\rho > 10^9$ Ω cm at 300 K for detectors with ohmic contacts has been developed. However, the leakage current in these detectors at room temperature is too large, which precludes a high-energy resolution in the measured spectra of *x*- and $\gamma$-rays. At the beginning of the 1990s, $Cd_{1-x}Zn_xTe$ alloy with a wider band gap and $\rho > 10^{10}$–$10^{11}$ Ω cm ($x = 0.1$–$0.2$) was proposed to be applied in the detectors of *x*- and $\gamma$-rays with the aim to provide lower leakage currents at higher voltages. Unfortunately, hopes for $Cd_{1-x}Zn_xTe$ were not fully justified. A search of the materials for semiconductor detectors for *x*- and $\gamma$-rays has continued. Among such materials, another CdTe-based alloy, $Cd_{1-x}Mn_xTe$ is considered as a promising material for *x*- and $\gamma$-ray detectors [1–3]. When growing $Cd_{1-x}Mn_xTe$ crystals, the segregation phenomena (causing a serious problem in $Cd_{1-x}Zn_xTe$ technology) manifest themselves as much weaker. In addition, the indispensable widening of the bandgap is achieved at a lower content of Mn. Due to these circumstances, the technology of growing homogeneous $Cd_{1-x}Mn_xTe$ crystals is simplified and becomes less expensive.

One of the first studies of $Cd_{1-x}Mn_xTe$ as a material for *x*- and $\gamma$-ray detectors was performed at the end of the 1990s [1]. It was established, and later confirmed by other studies, that the product of mobility $\mu$ and lifetime of electrons $\tau$ for the $Cd_{0.87}Mn_{0.13}Te$ crystals is close to the value of the best CdTe detectors ($\sim 10^{-3}$ cm$^2$ V$^{-1}$) [4, 5]. However, the resistivity of CdMnTe is usually close to $10^{10}$ Ω cm at 300 K, i.e., just a little higher than that of CdTe and the energy resolution in the recorded spectra is rather low (for example, 12.5% of the $^{241}$Am isotope at 59.5 keV peak) [1, 5].

 

In the late 1990s, new concepts of the detectors based on CdTe crystals with Schottky contacts and low leakage currents at high voltages were introduced [6, 7]. However, the fabrication of the diode structures based on $Cd_{1-x}Mn_xTe$ has not been successful. To date, there are very few publications devoted to the diodes based on $Cd_{1-x}Mn_xTe$ crystals. The Schottky diodes fabricated using n-type CdMnTe films grown by molecular beam epitaxy (MBE) on CdTe and CdZnTe substrates were investigated back in 1988 [8]. In 2010 and 2013, thin film p-ZnTe/n-CdMnTe/n-GaAs and CdTe/CdMnTe heterostructures were also grown by MBE [9, 10]. Such structures are of little interest for the detectors due to very low thickness of the CdMnTe films. Studies of Schottky diodes based on p-CdMnTe crystals are presented in a paper published in 2008 [11]. The barrier height at Al/p-CdMnTe Schottky contact was quite high, amounting to 0.8–0.88 eV. In the paper, electrical characteristics of the diodes are described briefly, and it is noted that for practical applications of Al/p-CdMnTe diodes further developments are required.

In this paper, the first Schottky diodes based on n-CdMnTe crystals having rectifying properties and low reverse currents at low bias voltages are investigated. Voltage dependences of current and their temperature changes are described analytically in terms of the generation–recombination mechanism in the space charge region (SCR) of the graphite/CdMnTe diode structure. The reasons for increasing the leakage currents in these structures at higher voltages are clarified and ways for their elimination are suggested.

## 2. Experimental results and discussion

For this study, n-type $Cd_{1-x}Mn_xTe$ ($x = 0.1$) crystals grown by a modified Bridgman method were used. The resistivity of the crystals at room temperature lies within the range $10^5$–$10^6$ Ω cm. The value $x = 0.1$ corresponds to the band gap $E_g = 1.47 + 1.45x = 1.62$ eV at 300 K [12, 13]. To account for the temperature variation of $E_g$ in the calculations, we will use, similarly to CdTe, the expression $E_g(T) = 1.767 - 4.91 \cdot T$, which gives $E_g = 1.62$ eV at 300 K.

Schottky diodes were fabricated by printing colloidal graphite on the CdMnTe surface at room temperature. A drop of colloidal graphite suspension was deposited with a teflon rod and left to dry (for more details see our previous papers [14, 15]. The contact area was checked by optical microscopy to maintain the contact sizes close to 1 mm. Prior to the graphite deposition, the surface of CdMnTe was etched in 0.1% bromine–methanol solution for 30 s (when the surface treatment was restricted only to cleaning in boiling methanol for 2 min, qualitatively different results, presented in section 2.4, were obtained). An ohmic contact on the back side of the crystal plate was formed by rubbing liquid gallium–indium alloy with a tin rod. The thickness of crystal was 0.7 mm.

As can be seen in figure 1, the *I–V* curve of the graphite/CdMnTe contact is characteristic for a semiconductor diode. The sample shows pronounced rectifying properties. It is sown in figure 1(*b*) that under forward bias the current follows the dependence $I = I_o[\exp(qV/nkT) - 1]$ (for $n \approx 2$ and $I_o = 1.2 \times 10^{-10}$ A) in the range of almost three orders of magnitude. This behavior is typical for semiconductor diodes with the recombination charge transport mechanism.

The deviation of the diode *I–V* curve from the exponential dependence is usually attributed to the influence of the series resistance of the bulk part of the crystal. Information about this resistance is provided by the voltage dependence of the differential resistance $R_{\text{dif}} = \mathrm{d}V/\mathrm{d}I$ of the diode under forward bias at different temperatures (figure 2). As can be seen, in the range of $V < 1$ V the differential resistance $R_{\text{dif}}$ rapidly decreases with voltage, while at $V > 1$ V the $R_{\text{dif}}$ value is practically unchanged. This behavior of $R_{\text{dif}}$ is explained by the fact that under forward biases the built-in potential $V_{\text{bi}} = \varphi_{\text{bi}}/q$ is compensated by the applied voltage, where $\varphi_{\text{bi}}$ is the height of the barrier caused by the band bending near the semiconductor surface.

At a sufficiently large forward voltage, the band bending practically disappears, the SCR closes up, and the voltage drop across the resistance of the crystal takes place. Under such conditions $R_{\text{dif}}$ is constant, and the dependence of current on voltage is linear. The fact that $R_{\text{dif}}$ at high voltages corresponds to the resistance of the crystal $R_{\text{ser}}$ is confirmed by the temperature dependence of the resistivity $\rho$ ($T$) found from the value of $R_{\text{dif}}$ at $V = 20$ V in figure 2(*a*), from the area of the graphite contact and from the thickness of the crystal. Such dependence of $\rho$ on $T$, given in figure 2(*b*), is similar to the dependence obtained from the resistivity measurements of specimens cut from the same ingot of CdMnTe.

### 2.1. Correlation of *I–V* characteristics with generation–recombination theory

It is known that the *I–V* characteristics of Schottky diodes based on CdTe can be well described by the generation–recombination in the SCR according to the theory of Sah–Noyce–Shockley [16]. It can also be assumed that such a mechanism of charge transport takes place in the graphite/CdMnTe Schottky diode, since there are a large number of deep levels in the band gap of CdMnTe (like in CdTe), which are effective centers of generation–recombination of charge carriers.

According to the Sah–Noyce–Shockley theory, the rate of recombination in the SCR under forward bias and generation under reverse bias are given by [16]:

$$U(x, V) = \frac{n(x, V)p(x, V) - n_{\text{i}}^2}{\tau_{\text{po}}[n(x, V) + n_1] + \tau_{\text{no}}[p(x, V) + p_1]}, \qquad (1)$$

where $n(x,V)$ and $p(x,V)$ are the carrier concentrations in the conduction band and in the valence band within the SCR, respectively; $n_i$ is the intrinsic carrier concentration in the semiconductor; $\tau_{\text{no}}$ and $\tau_{\text{po}}$ are the lifetimes of electrons and holes in highly p-type and highly n-type semiconductor, respectively. The quantities $n_1$ and $p_1$ in equation (1) are determined by the ionization energy of the generation–recombination center $E_t$: $n_1 = N_c \exp[-E_t/kT]$, $p_1 = N_v \exp(-(E_g - E_t)/kT)$, where $E_t$ is measured from the bottom of the conduction band; $N_c = 2(m_n \kappa T/2\pi\hbar^2)^{3/2}$ and $N_v = 2(m_p \kappa T/2\pi\hbar^2)^{3/2}$ are the effective densities of states in the

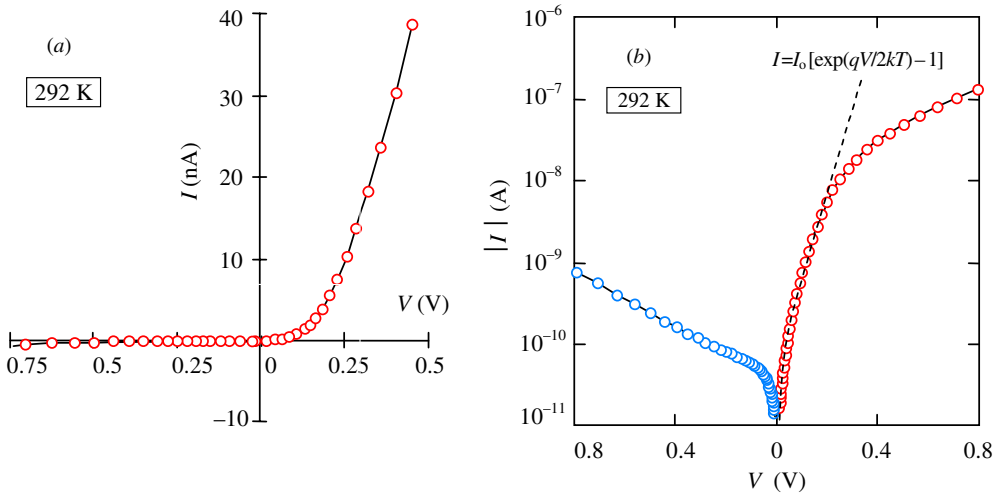


**Figure 1.** Room temperature *I–V* characteristics of semimetal graphite/CdMnTe Schottky diode shown in the linear (*a*) and semilogarithmic (*b*) plots.

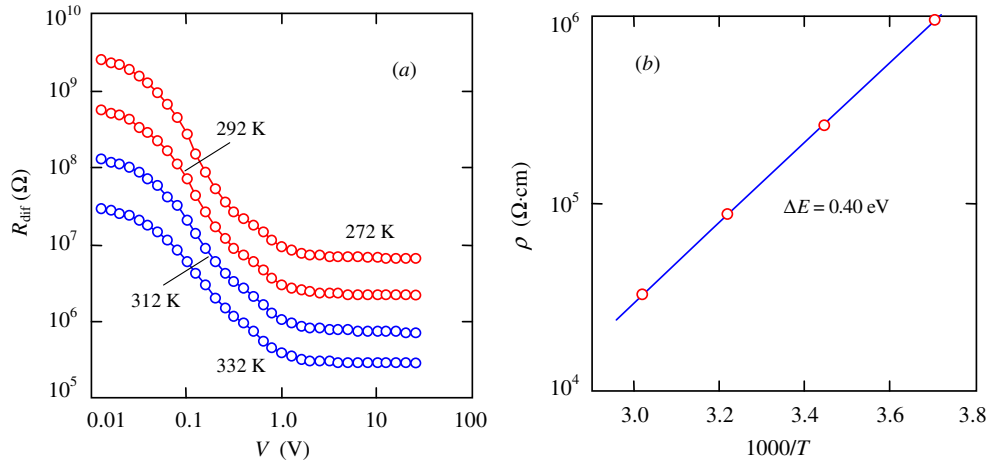


**Figure 2.** Voltage dependences of the differential resistance of the graphite/CdMnTe diode under forward biases at different temperatures (*a*) and temperature dependence of resistivity of the CdMnTe crystal (*b*).

conduction band and in the valence band, and $m_n$ and $m_p$ are the effective electron and hole masses, respectively.

The expressions for the electron and hole concentrations in the SCR of a Schottky diode take the form [17]:

$$n(x, V) = N_c \exp\left[-\frac{\Delta\mu + \varphi(x, V)}{kT}\right], \quad (2)$$

$$p(x, V) = N_v \exp\left[-\frac{E_g - \Delta\mu - \varphi(x, V) - qV}{kT}\right], \quad (3)$$

where $\Delta\mu$ denotes the energy gap between the Fermi level and the conduction band bottom in the bulk (neutral) part of the CdTe layer.

The potential energy in the SCR of Schottky diode is described by the parabolic law [18]

$$\varphi(x,V) = (\varphi_{bi} - qV)\left(1 - \frac{x}{W}\right)^2, \quad (4)$$

where $W$ is the width of the SCR:

$$W = \sqrt{\frac{2\varepsilon\varepsilon_o(\varphi_{bi} - qV)}{q^2(N_d - N_a)}}, \quad (5)$$

$\varepsilon$ is the relative permittivity of semiconductor, $\varepsilon_o$ is the permittivity of vacuum, $N_d - N_a$ is the concentration of uncompensated donors in the CdTe layer, $\varphi_{bi}$, as before, is the height of potential barrier from the side of the semiconductor. It should be noted that, in contrast to the mechanism of thermionic emission, where the main barrier for the charge carriers is $\Phi_b = \varphi_{bi} + \Delta\mu$, the barrier height $\varphi_{bi}$ is one of the key parameters that determines the generation–recombination processes in the SCR of Schottky diode (the barrier $\Phi_b$ does not appear in the generation–recombination theory).

The generation–recombination current density is found by integration of $U(x,V)$ over the SCR:

$$J = q\int_0^W U(x, V)\,dx. \quad (6)$$

A comparison of the *I–V* characteristics of the graphite/CdMnTe contact with the experimental data calculated for different temperatures is shown in figure 3. In the calculations, voltage drop across the series resistance of the crystal bulk $R_{ser}$ was taken into account, which affected the current only at high forward bias. The Fermi level energy

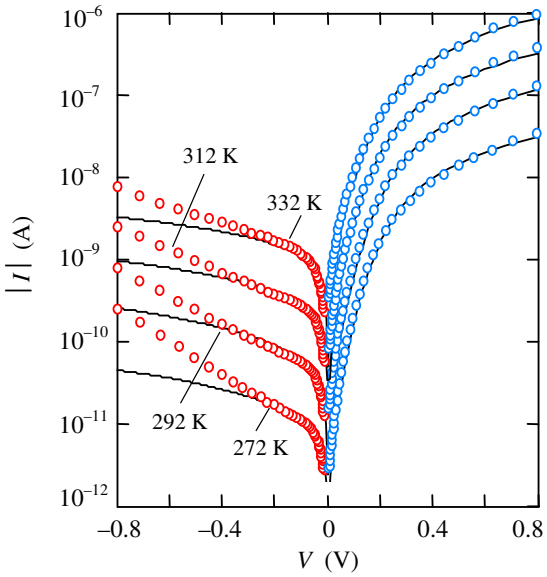


**Figure 3.** Comparison of the calculation results (solid lines) with the *I–V* characteristics of the graphite/CdMnTe diode measured at different temperatures (circles).

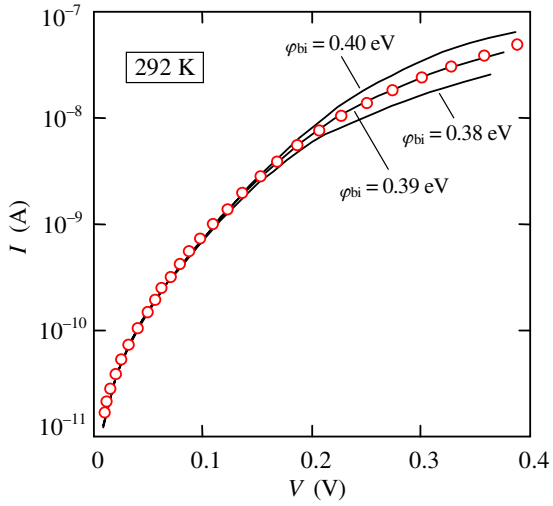


**Figure 4.** Comparison of the experimental data on the forward current at 292 K with the curves calculated for different barrier heights.

$\Delta\mu$, required for calculation of the *I–V* characteristic, can be found from the data shown in figure 2. Knowing the resistivity $\rho$, one can find the concentration of free electrons as $n = 1/q\rho\mu_n$ and then the energy of the Fermi level as $\Delta\mu = kT\ln(N_c/n)$ (0.532 eV at 292 K, for example) accepting $\mu_n = 720$ cm$^2$ (V s)$^{-1}$ [19].

According to the theory, apart from the Fermi level energy $\Delta\mu$, the forward current is also determined by the $[\tau_{no}\tau_{po}(N_d - N_a)]^{1/2}$ value [17]. In the calculations, the concentration of uncompensated donors was initially assumed to be $10^{16}$ cm$^{-3}$ (even in pure CdTe crystals, and the more so in the CdMnTe, the concentration of residual impurities may reach $10^{15}$–$10^{16}$ cm$^{-3}$). Specifying the value $N_d - N_a$, it is easy to justify $(\tau_{no}\tau_{po})^{1/2}$ such that the calculated and measured forward currents coincide. To have the right value of the *forward* current, the values of $[\tau_{no}\tau_{po}]^{1/2}$ should be $(0.7 \pm 0.5) \times 10^{-12}$ s.

The value of the *reverse* current is mainly determined by the energy of generation–recombination center $E_t$. Best agreement of the calculated results and the measured reverse current is achieved, when $E_t = 0.69 \pm 0.01$ eV for all temperatures, i.e., if the level of the center is located near the middle of the band gap, as it should be according to the Shockley–Read–Hall statistics.

The barrier height $\varphi_{bi}$ affects the forward *I–V* characteristic only at high *V*, and therefore the value of $\varphi_{bi}$ can be matched by fitting the calculation results with the experimental data on the last stage of the parameter choice. For the best match between the theory and experiment at 292 K, the values of the barrier height $\varphi_{bi}$ were taken equal to 0.39 eV. Figure 4 demonstrates a method to determine the $\varphi_{bi}$ value by comparing the calculation results of the forward current with the experimental data obtained at 292 K (taking into account the voltage drop across the series resistance $R_s$). As seen, a change in the value of $\varphi_{bi}$ by 0.01 eV causes a significant deviation of the calculated curve from the experimental points, i.e., this method provides a sufficiently accurate determination of the barrier height. This is important because conventional methods, for example by means of *C–V* measurements, is very complicated due to the presence in the electrical circuit of large series resistance $R_s = 10^5$–$10^7$ Ω (figure 2). For the same reason, the creation of flat-band condition to determine the barrier height is also difficult, because when *V* approaches $V_{bi} = \varphi_{bi}/q$, a significant voltage is dropped on the crystal and the electric field in it is not zero.

As can be seen in figure 3, the Sah–Noyce–Shockley theory describes well the forward *I–V* characteristic of the studied graphite/CdMnTe diode. According to the theory, the voltage dependence of the forward recombination current is described by function $\exp(qV/nkT)$–1 ($n \approx 2$), but only at a voltage lower than $V = (1/q)|2(\varphi_{bi} + \Delta\mu) - E_g|$, i.e., at $V <$0.22–0.24 V, as observed in the experimental curves in figure 1(*b*) [17]. Thus, the low barrier height $\varphi_{bi}$ explains the absence of the lengthy straight line section on the dependence of $\log I$ on *V* under high forward biases. The barrier height $\varphi_{bi}$ can be increased by reducing the resistivity of the crystal and hence nearing the Fermi level to the conduction band. If, for example, $\varphi_{bi}$ is raised to 0.9 eV, one can obtain the extended exponential plot $I \propto \exp(qV/nkT)$ on the $I(V)$ dependence and the current of 5–6 mA at 0.8 V.

The forward *I–V* characteristic is not so important for applications in the *x*- and $\gamma$-ray detectors. The value of reverse current is more significant from this point of view. As seen in figure 3, the theory reproduces well the reverse *I–V* characteristic of the diode when a bias is lower than $\sim$ 0.3 V. However, at a larger voltage, another charge transport mechanism manifests itself resulting in additional current that will be discussed in the next section.

The changes of the electrical characteristics with temperature of the graphite/CdMnTe diode confirm the above conclusion that the main charge transport mechanisms are the generation–recombination processes in the SCR. Figure 5 shows the temperature dependences of the reverse current

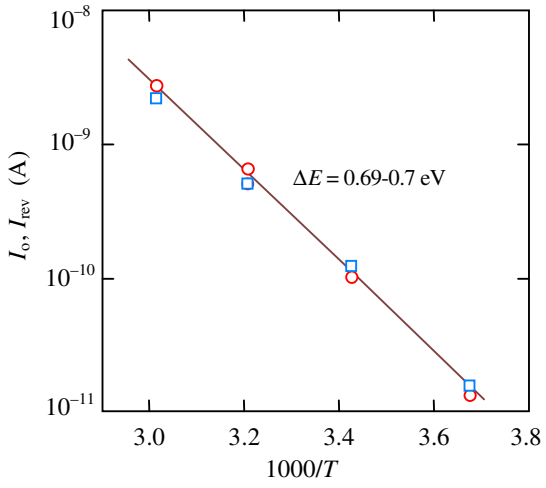


**Figure 5.** Temperature dependences of the reverse current $I_{rev}$ at $V = -0.2$ V (circles) and the saturation current $I_o$ obtained from the forward current (squares).

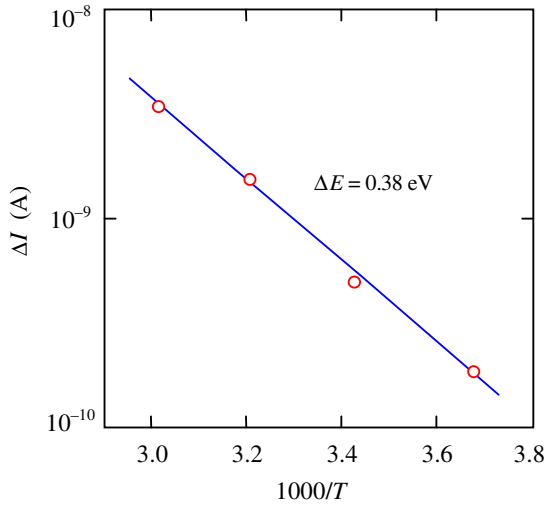


**Figure 6.** Temperature dependence of the current $\Delta I$ excessive over the generation current under reverse bias.

$I_{rev}$ at $V = -0.2$ V and the so-called saturation current $I_o$ in the expression for the forward current in the form $I = I_o[\exp(qV/1.9kT)-1]$.

As seen in figure 5, in agreement with the theory, the thermal activation energy $\Delta E = 0.69$–$0.7$ eV of both direct and reverse currents are very close to each other and correspond to the level located near the middle of the band gap of the semiconductor being distant from it only by about 0.1 eV.

### *2.2. Tunneling currents under reverse bias*

As seen in figure 3, an additional charge transport mechanism manifests itself at the reverse voltage above 0.2–0.3 V, which is excessive over the generation current. A characteristic feature of this current is that the $I(V)$ dependence is super-linear, which contradicts the thermal generation mechanism of charge carriers. The excessive current $\Delta I$ found as the difference between the measured current $I$ and the calculated generation current $I_g$ at $V = 0.8$ V increases with increasing temperature (see figure 6) although its activation energy (0.38 eV) is considerably smaller than that of the generation current measured at the voltage lower than 0.3 V (0.69–0.7 eV).

The image-force lowering can lead to the thermionic emission current increase with temperature and bias voltage in Schottky diodes. However, the value of this lowering in our case $\Delta\varphi = q[q2(\varphi_{bi} - qV)/4\pi\varepsilon\varepsilon_o W)]^{1/2}$ is equal to 0.032 eV at $V = -0.2$ V and increases to 0.033 eV at $V = -0.8$ V. With allowance for this Schottky effect, the thermionic emission current becomes equal to $A^*T^2\exp[-(\varphi_{bi} + \Delta\mu - \Delta\varphi)/kT]$, where $A^* = 4\pi qm_n k^2/h^3$ is the effective Richardson constant. By substituting for $m_n$, $\varphi_{bi}$, $\Delta\mu$, $\Delta\varphi$ one obtains the current value, which is 2–3 orders of magnitude lower than the measured current at all temperatures. Thus, the thermionic emission cannot explain the observed increase in the reverse current at $V > 0.2$–$0.3$ V.

The temperature variation of the excessive current $\Delta I = I - I_g$ shown in figure 6 is not consistent with the avalanche processes, because as the temperature increases, the impact ionization is weakened rather than strengthened. In addition, the impact ionization cannot start at the voltage of 0.2–0.3 V. Thus, one has to assume that an increase in the reverse current is caused by tunneling of electrons through the barrier region, which is possible if the barrier width is thin enough.

The tunneling current in a Schottky diode is usually represented as [18]:

$$I_{tun} = I_{to}\frac{\varphi_{bi} - qV}{\varphi_{bi}}\exp\left(-\frac{4}{3\hbar}\sqrt{\frac{m_n\varepsilon\varepsilon_o}{N_d - N_a}}\frac{\varphi_{bi}^{3/2}}{\sqrt{\varphi_{bi} - qV}}\right), \quad (7)$$

where $I_{to}$ is the coefficient independent of $V$, other notations are the same as earlier.

The voltage dependence of the excess current $\Delta I$ measured at 292 K and the current calculated by equation (7) are shown in figure 7 by circles and a solid line, respectively. The data are presented in the coordinates commonly used for the tunneling current, i.e., as $\Delta I/(\varphi_{bi} - qV)$ versus $1/\sqrt{\varphi_o - qV}$. As can be seen, the voltage dependence of current $\Delta I$ agrees very well with equation (7) for the tunneling current in the whole range of its change.

From the slope of the resulting straight line in figure 7(*b*) it follows that the concentration of uncompensated donors in the CdMnTe crystal is equal to $7 \times 10^{17}$ cm$^{-3}$. According to equation (5) at $\varphi_{bi} = 0.4$ eV, this corresponds to the width of the SCR at zero bias $W \approx 0.03$ $\mu$m, i.e., the barrier width in graphite/CdMnTe Schottky diode is indeed very small. However, if the SCR is sufficiently narrow, the tunneling of electrons occurs mainly from the levels in metal located near or below the Fermi level, and then the tunneling current is practically independent of temperature. Let us consider the energy distribution of tunneling electrons in the Schottky diode under study in order to explain significant temperature variations of current $\Delta I$ presented in figure 6.

For the tunneling probability one can use the expression known from quantum mechanics:

$$D(E) = \exp\left(-\frac{2\sqrt{m_n}}{\hbar}\int_0^{x_2}\sqrt{\varphi(x,V) - E}\,dx\right), \quad (8)$$

where $\varphi(x,V)$ is the potential energy distribution given by equation (4), $E$ is the energy of tunneling electron, $x_2$ is the

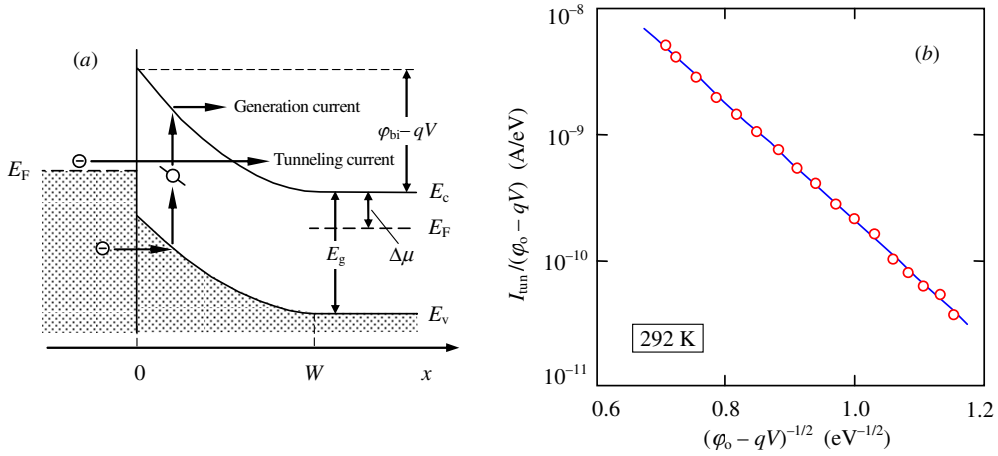


**Figure 7.** (*a*) Energy band diagram of the graphite/CdMnTe diode. (*b*) Comparison of the voltage dependence of the current $\Delta I$ excessive over the generation current at 332 K with equation (7) for tunneling current.

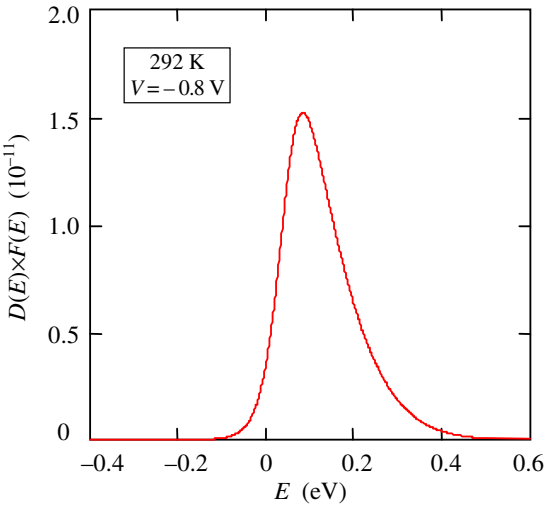


**Figure 8.** Energy distribution of electrons tunneling in the graphite/CdMnTe Schottky diode at $V=-0.8$ V.

coordinate, which can be found from the condition $\varphi(x_2,V) - E = 0$. The width of the SCR $W$ appearing in $\varphi(x,V)$ is determined by equation (5) for $N_d - N_a = 7 \times 10^{17}$ cm$^{-3}$.

Distribution of tunneling electrons can be found by multiplying $D(E)$ by the Fermi–Dirac distribution function $F(E)$. Relative to the Fermi level in the metal, one can write for $F(E)$:

$$F(E) = \frac{1}{1+\exp(E/kT)}. \tag{9}$$

The calculation results of energy distribution of electrons tunneling through a barrier for reverse bias 0.8 V using equations (4), (5), (8) and (9) are shown in figure 8.

As seen in figure 8, the distribution maximum of tunneling electrons falls on the energy $\sim 0.08$ eV above 0, but electrons tunnel through the barrier also at higher energies up to $E \approx 0.4$ eV. With increasing $T$, the number of electrons tunneling with energy above zero increases, which explains the observed increase of tunneling current with temperature shown in figure 3.

### *2.3. Compensation degree of the material and related technological problems*

A high concentration of uncompensated donors is not acceptable for using the CdMnTe crystals in detectors of $x$- and $\gamma$-rays, because the most active area of the crystal (which is the SCR) is too thin in this case and hence the detection efficiency is low. In addition, as is shown above, the narrowness of the SCR causes the super-linear increase in diode reverse current (the leakage current of the detector), which is also highly undesirable.

Let us analyze the conditions which cause a sufficiently high resistivity state of the material $2 \times 10^5$ Ω cm at 292 K and, at the same time, a high concentration of uncompensated donors $7 \times 10^{17}$ cm$^{-3}$.

Such a high concentration of uncompensated donors is consistent with the analysis of the electrical characteristics of CdMnTe crystal. The above temperature dependence of the resistivity $\rho$ (figure 2(*b*)) allows us to find the concentration of electrons in the conduction band $n$, and then the energy of the Fermi level $\Delta\mu = kT\ln(N_c/n)$. The obtained temperature dependence of $\Delta\mu$ is shown in figure 9 by circles. Since CdMnTe crystal is undoubtedly a compensated semiconductor, an insignificant change in the position of the Fermi level with temperature indicates the dominant role of the deep donor in determining the electrical conductivity of the material.

Denote the concentration and ionization energy of introduced donors by $N_d$ and $E_d$, respectively. Considering the statistics of charge carriers, it is necessary to include acceptors in consideration, the concentration of which we denote by $N_a$. Assume also that the acceptor levels are located in the lower half of the band gap, i.e., almost all acceptors are ionized (are negatively charged). Electroneutrality condition for such a semiconductor apparently has the form:

$$n + N_a = N_d^+, \tag{10}$$

where $N_d^+$ is the concentration of charged donors.

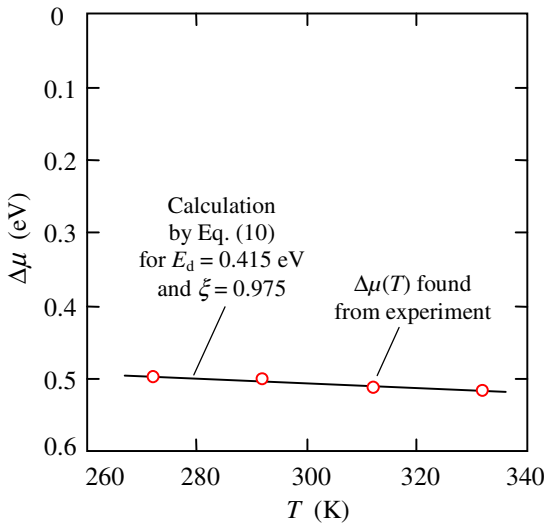


**Figure 9.** Position of the Fermi level in the band gap of CdMnTe crystal as a function of temperature.

The donor level may be near the Fermi level, so in the expression for concentration of charged donors $N_d^+$ one should use the Fermi–Dirac statistics:

$$N_d^+ = \frac{N_d}{\exp\left(\frac{E_d - \Delta\mu}{kT}\right) + 1}. \tag{11}$$

The concentration of electrons in the conduction band $n = 1/q\rho\mu_n$ even at the highest temperature (332 K) does not exceed $10^{11}$ cm$^{-3}$, therefore $n$ can be neglected in equation (10), and then the solution of the electroneutrality equation $N_a = N_d^+$ with respect to $\Delta\mu$ has the form:

$$\Delta\mu = E_d - kT \ln\left(\frac{1-\xi}{\xi}\right), \tag{12}$$

where $\xi = N_a/N_d$ is the compensation degree of donor impurities.

Figure 9 shows a comparison of the calculation results (solid line) of $\Delta\mu$ using equation (12) for $E_d = 0.415$ eV and $\xi = 0.975$ with the temperature variation of $\Delta\mu$ found from the experimental data (circles) for $\rho$ shown in figure 2(*b*). Note that to adjust $E_d$ and $\xi$ for the best match between theory and experiment is easy, since the variation of $E_d$ practically results only in a shift along the vertical axis, while the $\xi$ affects mainly the slope of the straight line.

From the comparison between theory and experiment, it follows that the conductivity of the crystals is determined by the deep levels ($E_d = 0.415$ eV) of highly compensated impurity ($\xi = 0.975$). In our previous publication [20], it was shown that the doping of CdTe with Mn leads to similar results. We can therefore assume that in the CdMnTe crystals, a certain part of Mn atoms does not substitute for Cd, but plays a role of over-stoichiometric impurity. Manganese, similarly to other elements of group VII of the periodic table (Cl, In, Br, I), is apparently a self-compensating impurity, which explains the high degree of compensation of CdMnTe crystals under study.

It seems that these results reveal some important *aspects concerning the technology* of growing and post-processing CdMnTe crystals.

Knowing the uncompensated donor concentration $N_d - N_a = 7 \times 10^{17}$ cm$^{-3}$ (found from the tunneling current in the diode) and the degree of compensation $\xi = N_a/N_d = 0.975$, one can determine the concentration of over-stoichiometric manganese $N_d = (N_d - N_a)/(1 - \xi) = 2.8 \times 10^{19}$ cm$^{-3}$ and the concentration of acceptors (defects) arisen as a result of the formation of complexes due to doping with the element of group VII of the periodic table $N_a = (N_d - N_a)\xi/(1 - \xi) = 2.73 \times 10^{19}$ cm$^{-3}$. To widen the SCR and thereby reduce tunneling, it is necessary to increase the degree of compensation of donors and hence to decrease $N_d - N_a$. In order to have, for example, at $V = 10$ V the same tunneling current as at 0.3 V and $N_d - N_a = 7 \times 10^{17}$ cm$^{-3}$, the concentration of uncompensated donors must be reduced according to equation (7) to $2.203 \times 10^{16}$ cm$^{-3}$. For this purpose, an additional acceptor impurity with a concentration of $6.779 \times 10^{17}$ cm$^{-3}$ should be introduced into the CdMnTe crystal. In order to have the same tunneling current at $V = 100$ V and 400 V, the concentration of additional acceptors should be $6.9821 \times 10^{17}$ and $6.9961 \times 10^{17}$ cm$^{-3}$, respectively.

As seen, the desired extension of the SCR from 0.03 to $\sim 1$ $\mu$m (at zero bias) occurs when the concentration of additional acceptor impurities varies in an extremely narrow range of $6.779 \times 10^{17}$ to $6.9961 \times 10^{17}$ cm$^{-3}$. Deviation of the concentrations of acceptors upward or downward only by 0.01%, in the case of the width of the SCR providing elimination of tunneling at the bias voltage of 400 V, causes a change in the tunneling current of $\sim 4$ and $\sim 5$ times, respectively! With the expansion of the SCR, the concentration of additional acceptors closely approaches the value of $N_d - N_a = 7 \times 10^{17}$ cm$^{-3}$. If the concentration of acceptors even slightly exceeds $N_d - N_a$, the conductivity type of semiconductor is converted and the contact ceases to be a Schottky diode. Apparently, to set the concentration of additional acceptor impurities across the whole crystal with such precision is unrealistic. It seems that a more realistic way to solve the problem is by growing the crystals of stoichiometric composition, for which the accuracy requirements to maintain the concentration of the dopant are not so stringent.

It is also desirable to dope the material with self-compensating impurity, the level of which is located *near the midgap* rather than with the ionization energy $E_d = 0.415$ eV found above. In this case, it is possible to obtain *a semi-insulating material with a required low concentration of uncompensated impurity* (as occurs in Cl-doped CdTe crystals [21]).

### *2.4. Currents caused by the Frenkel–Poole emission*

As expected, the special treatment of the CdMnTe crystal surface before the application of colloidal graphite has a considerable influence on the properties of contacts. If the pretreatment does not include certain $C_2H_5BrO$ processing, the *I–V* characteristic of the graphite/CdMnTe contact becomes qualitatively different from the results shown so far. As in the case of the diode structure, the current at different polarities of

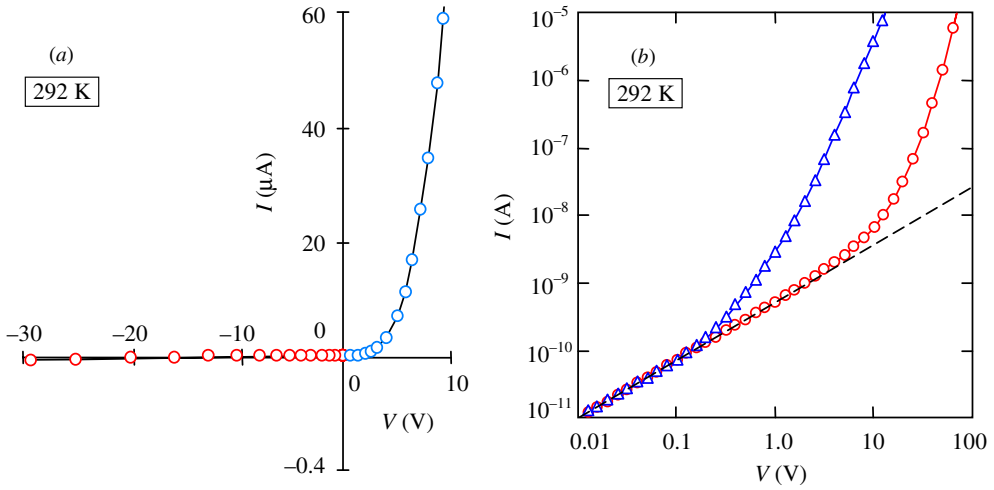


**Figure 10.** *I–V* characteristics of graphite/CdMnTe contact in linear (*a*) and double-logarithmic (*b*) coordinates fabricated without processing by $C_2H_5BrO$ of the crystal surface prior to the application of graphite. The dashed straight line shows the linear approximation.

the applied voltage are significantly different. However, this only holds for larger voltages of several volts, as shown in figure 10(*a*). At lower voltages (<0.2–0.3 V) the current for both polarities is practically the same and depends linearly on the applied voltage. Such properties are unnatural for a semiconductor diode with a Schottky contact or a p–n junction.

It is known that crystals with ohmic contacts show similar characteristics when at larger voltages the space charge limited (SCL) currents come into play. In our case such a charge transport mechanism can be excluded, since the SCL currents are only significant when the concentration of injected charge carriers from the contact exceeds the concentration of equilibrium free carriers (for the formation of an appreciable space charge). In our case, the concentration of electrons in the conduction band $n = 9 \times 10^{10}$ cm$^{-3}$ at 300 K is apparently too high to explain the deviation from a linear dependence of $I$ above 0.1 nA (figure 10(*b*)). In addition, the quadratic dependence $I \propto V^2$, which is characteristic of the SCL current, cannot be seen in the measured curve at larger $V$. Instead, a sharp *exponential* dependence of $I$ versus $V$ without any tendency to the quadratic law is observed.

The experimental data shown in figure 10 can be explained by assuming that without the $C_2H_5BrO$ pretreatment, the *I–V* characteristic is controlled by a thin insulating oxide layer between the graphite and CdMnTe crystal. The oxide presence is indicated primarily by the fact that, at low voltage, the current through the sample at room temperature is more than two orders of magnitude higher than that calculated for the crystal with ohmic contacts ($\rho = 2 \times 10^6$ cm Ω).

The relatively high electrical conductivity of the oxide layer at high voltages can be explained by the Frenkel–Poole transport mechanism [22] widely used to interpret the characteristics of metal–insulator–semiconductor (MIS) structures [18]. According to this transport model, the conductivity of the insulating film in the MIS structure is determined by the thermal excitation of electrons from the trapping levels in the band gap of the insulator, therefore its temperature dependence is described by the factor $\exp(-E_t/kT)$, where $E_t$ is the ionization energy of the trap (capture center) in zero electric field. The electric field in a thin-film insulator even under moderate voltage is high. As a result, the height of the potential barrier for electrons at the capture center is reduced and thermal excitation of electrons is enhanced.

For the trap states with Coulomb potential, the expression for the current density in the insulator with its thickness $d$ can be represented as [18]:

$$J = q\mu_n \frac{V}{d} N_c \exp\left(-\frac{E_t}{kT}\right) \exp\left(\frac{q\sqrt{qV/\pi\varepsilon\varepsilon_o d}}{kT}\right), \qquad (13)$$

where the last factor takes into account the decrease of the barrier by an electric field, for which the square root dependence on the voltage in the exponent is a characteristic of the Frenkel–Poole emission (the electric field is assumed to be uniform and equal to $V/d$).

Figure 11(*a*) shows a comparison of equation (13) with the *I–V* characteristic of the graphite/CdMnTe contact fabricated without the $C_2H_5BrO$ crystal pretreatment for the polarity of the applied voltage corresponding to smaller currents at high voltages. Comparison is made at larger voltages, where the Frenkel–Poole effect dominates in charge transport. As usual, the coordinates have been selected such that a straight line in accordance with equation (13) is obtained. As can be seen, the experimental data agree very well with the above assumption that the rapid increase of the current at larger voltages is caused by the Frenkel–Poole emission. This conclusion is also confirmed by the temperature dependence of the current shown in figure 11(*b*) for the same polarity.

The thermal activation energy of the current found from the slope of the straight lines obtained at a voltage of 3 V, where the conductivity of a thin insulating oxide layer is determined by the thermal excitation of electrons without the involvement of an electric field $E_t$ is equal to 0.63 eV. However, at a voltage of 100 V, where the Frenkel–Poole emission dominates, the thermal activation energy equals 0.26 eV. This energy is obviously equal to the ionization energy of the trap under the conditions of an electric field acting in the oxide layer. The difference between these energies 0.37 eV is equal

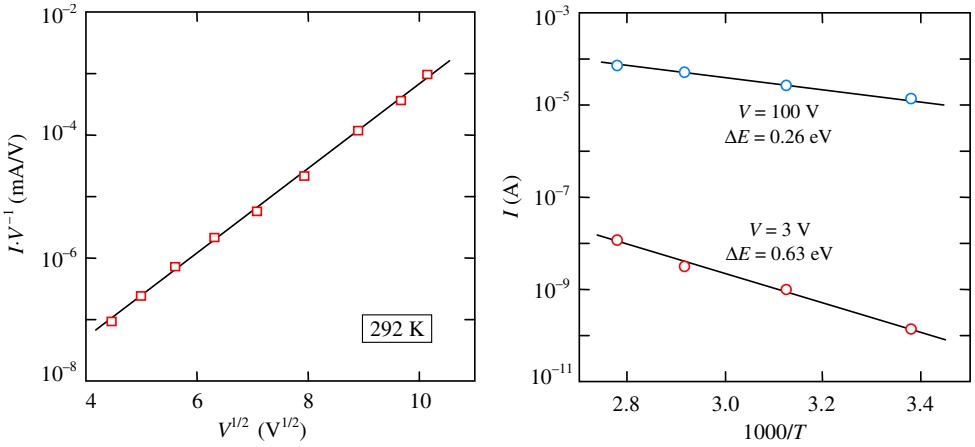


**Figure 11.** (*a*) Comparison *I–V* characteristic of the crystal without the surface treatment in $C_2H_5BrO$ with equation (13) at $V > 20$ V at two polarities of applied bias voltage. (*b*) Temperature dependences of the current at two applied voltages.

to the lowering of the barrier for electrons on the trap, which according to the theory is $(q^3V/\pi\varepsilon\varepsilon_o d)^{1/2}$ [18]. This implies that the thickness of the insulating film between the graphite and the CdMnTe crystal is equal to 0.41 $\mu$m.

Ohmic behavior and Poole–Frenkel emission observed in the oxide layer at low and high voltages, respectively, are similar to those which take place in the resistive film of integrated ZnO-based 1D1R switching devices developed for applications in reconfigurable electronics and nonvolatile memory [23, 24]. However, the resistive switching effect in the above discussed oxide layer is not observed.

## 3. Conclusions

The foregoing results show that the problem of the fabrication of a diode structure based on n-type CdMnTe crystals can be overcome. Schottky diodes obtained by printing colloidal graphite on the pre-treated surface of the crystal exhibit pronounced rectifying properties.

(i) The *I–V* characteristics are well described by the Sah–Noyce–Shockley theory of generation–recombination in the SCR of the diode. Exponential increase of the forward current with the voltage is limited by a relatively low barrier height at the contact ($\sim$ 0.4 eV) and a significant series resistance of the crystal ($\sim 10^6$ $\Omega$ at room temperature).

(ii) The tunneling of electrons in the Schottky diodes under investigation (due to high concentration of uncompensated donors) limits the possibility for increasing the reverse bias voltage, which is necessary for the use of such diodes as detectors of *x*- and $\gamma$-radiation.

(iii) A high concentration of uncompensated donors $7 \times 10^{17}$ cm$^{-3}$ is explained by the fact that a certain part of Mn atoms does not substitute for Cd but plays the role of over-stoichiometric impurities.

(iv) Analysis of the avenues to reduce the concentration of uncompensated donors sheds light on the critical issues of CdMnTe crystal growth technology for *x*- and $\gamma$-ray detectors. To reduce the concentration of uncompensated donors by additional doping with acceptors is unrealistic, because a very high accuracy of the acceptor concentration is required.

(v) In the presence of a thin intermediate insulator layer in the graphite/CdMnTe contact, the current at a larger voltage is caused by the Frenkel–Poole emission for both polarities of the applied voltage.

## Acknowledgments

This research has been performed in the framework of the Collaborative Project COCAE SEC-218000 of the European Community's Seventh Framework Programme and project COST LD120014 of the Ministry of Education of the Czech Republic.

## References

[1] Burger A, Chattopadhyay K, Chen H, Ndap J O, Ma X, Trivedi S, Kutcher S W, Chen R and Rosemeier R D 1999 *J. Cryst. Growth* **198/199** 872
[2] Mycielski A, Burger A, Sowinska M, Groza M, Szadkowski A, Wojnar P, Witkowska B,, Kaliszek W and Siffert P 2005 *Phys. Status Solidi c* **2** 1578
[3] Hossain A, Cui Y, Bolotnikov A E, Camarda G S, Yang G, Kochanowska D, Witkowska-Baran M, Mycielski A and James R B 2009 *J. Electron. Mater.* **38** 1593
[4] Kim K, Cho S, Suh J, Hong J and Kim S 2009 *IEEE Trans. Nucl. Sci.* **56** 858
[5] Du Y, Jie W, Wang T, Zheng X, Xu Y and Luan L 2012 *J. Cryst. Growth* **355** 33
[6] Matsumoto C, Takahashi T, Takizawa K, Ohno R, Ozaki T and Mori K 1998 *IEEE Trans. Nucl. Sci.* **45** 428
[7] Takahashi T, Paul B, Hirose K, Matsumoto S, Ohno R, Ozaki T, Mori K and Tomita Y 1999 *Nucl. Instrum. Methods* A **436** 111
[8] Dreifus D L, Kolbas R M, Harper R L, Tassitino J R, Hwang S and Schetzina J F 1988 *Appl. Phys. Lett.* **53** 1279
[9] Yahia I S, Sakr G B, Wojtowicz T and Karczewski G 2010 *Semicond. Sci. Technol.* **25** 095001
[10] Yahia I S, Yakuphanoglu F, Chusnutdinow S, Wojtowicz T and Karczewski G 2013 *Curr. Appl. Phys.* **13** 537

[11] Zhang J, Jie W, Hao Y and Wang X 2008 *Semicond. Sci. Technol.* **23** 075010
[12] Bottka N, Stankiewicz J and Giriat W 1981 *J. Appl. Phys.* **52** 41
[13] El Amrani M, Lascaray J P and Diouri J 1983 *Solid State Commun.* **45** 351
[14] Yatskiv R and Grym J 2013 *Semicond. Sci. Technol.* **28** 055009
[15] Yatskiv R and Grym J 2012 *Appl. Phys. Lett.* **101** 162106
[16] Sah C T, Noyce R N and Shokley W 1957 *Proc. IRE* **45** 1228
[17] Kosyachenko L A, Maslyanchuk O L, Motushchuk V V and Sklyarchuk V M 2004 *Sol. Energy Mater. Sol. Cells* **82** 65
[18] Sze S M and Ng Kwok K 2006 *Physics of Semiconductor Devices* 3d edn (Hoboken, NJ: Wiley-Interscience)
[19] Rafiei R, Boardman D, Reinhard M I, Sarbutt Kim K, Watt G C, Uxa S, Prokopovich D A, Belas E, Bolotnikov A E and James R B 2012 *Records of EPJ Web of Conf. Symp. on Fundamental and Applied Science* vol 35 02005
[20] Kosyachenko L A, Yurtsenyuk N S, Rarenko I M, Sklyarchuk V M, Sklyarchuk O F, Zakharuk Z I and Grushko E V 2013 *Semiconductors* **47** 916
[21] Kosyachenko L A, Aoki T, Lambropoulos C P, Gnatyuk V A, Grushko E V, Sklyarchuk V M, Maslyanchuk O L, Sklyarchuk O F and Koike A 2013 *IEEE Trans. Nucl. Sci.* **60** 2845
[22] Frenkel J 1938 *Tech. Phys. USSR* **5** 685
[23] Chang W-Y, Lai Y-C, Wu T-B, Wang S-F, Chen F and Tsai M-J 2008 *Appl. Phys. Lett.* **92** 022110
[24] Zhang Y, Duan Z, Li R, Ku C-J, Reyes P I, Ashrafi A, Zhong J and Lu Y 2013 *J. Phys. D: Appl. Phys.* **46** 145101